

RADIO-CONTINUUM EMISSION FROM THE YOUNG GALACTIC SUPERNOVA REMNANT G1.9+0.3

A. Y. De Horta¹, M. D. Filipović¹, E. J. Crawford¹, F. H. Stootman¹, T. G. Pannuti²,
L. M. Bozzetto¹, J. D. Collier¹, E. R. Sommer¹ and A. R. Kosakowski²

¹*University of Western Sydney, Locked Bag 1797, Penrith South, DC, NSW 1797, Australia*
E-mail: a.dehorta@uws.edu.au, m.filipovic@uws.edu.au, e.crawford@uws.edu.au

²*Space Science Center, Department of Earth and Space Sciences, Morehead State University, 235 Martindale Drive, Morehead, KY 40351 USA*
E-mail: t.pannuti@moreheadstate.edu

(Received: June 5, 2014; Accepted: June 18, 2014)

SUMMARY: We present an analysis of a new Australia Telescope Compact Array (ATCA) radio-continuum observation of supernova remnant (SNR) G1.9+0.3, which at an age of $\sim 181 \pm 25$ years is the youngest known in the Galaxy. We analysed all available radio-continuum observations at 6-cm from the ATCA and the Very Large Array. Using this data we estimate a median expansion rate for G1.9+0.3 of $0.563\% \pm 0.078\%$ per year between 1984 and 2009. We note that in the 1980's G1.9+0.3 expanded somewhat slower (0.484% per year) than more recently (0.641% per year). We estimate that the average spectral index between 20-cm and 6-cm, across the entire SNR is $\alpha = -0.72 \pm 0.26$ which is typical for younger SNRs. At 6-cm, we detect an average of 6% fractionally polarised radio emission with a peak of $17\% \pm 3\%$. The polarised emission follows the contours of the strongest of X-ray emission. Using the new equipartition formula we estimate a magnetic field strength of $B \approx 273 \mu\text{G}$, which to date, is one of the highest magnetic field strength found for any SNR and consistent with G1.9+0.3 being a very young remnant. This magnetic field strength implies a minimum total energy of the synchrotron radiation of $E_{\min} \approx 1.8 \times 10^{48}$ ergs.

Key words. ISM: individual: G1.9+0.3 – supernova remnants – supernovae general – radio continuum.

1. INTRODUCTION

It is widely accepted that current catalogues have a distinct deficit of young Galactic supernova remnants (SNRs), that is, SNRs <2000 years old, with only ~ 10 confirmed out of a predicted ~ 50 (van den Bergh & Tammann 1991; Cappellaro 2003). Of these confirmed SNRs, G1.9+0.3 is of particular in-

terest as it is believed to be the youngest in the Milky Way (MW) at ~ 150 years old (Reynolds et al. 2008; Green et al. 2008; Reynolds et al. 2009; Carlton et al. 2011a,b).

Originally identified as a probable SNR by Green & Gull (1984) at 4.9 GHz using the Karl G. Jansky Very Large Array (VLA), G1.9+0.3 was described as a shell source with an approximate bright-

ness slightly less than that of the Tycho and Kepler SNRs with a spectral index of $\alpha \sim -0.7^1$. Using the Molonglo Observatory Synthesis Telescope (MOST) Galactic Survey data, Gray (1994) confirmed the classification of G1.9+0.3 as an SNR: the source was described as featuring a shell-like morphology in the radio with an estimated diameter of $1\frac{1}{2}$. Later, LaRosa et al. (2000) produced a 90-cm image of G1.9+0.3 made using observations from the VLA. They estimated the 20/90-cm spectral index of the SNR to be $\alpha = -0.93 \pm 0.25$ and the angular diameter to be $1\frac{1}{4}$. Nord et al. (2004) revisited the data collected by LaRosa et al. (2000) and – through the application of superior data reduction techniques – measured the diameter of G1.9+0.3 to be $<1'$ and placed it at a distance of <7.8 kpc. Green (2004) estimates the diameter of G1.9+0.3 based on 1.49 GHz VLA observations made in 1985 to be $1\frac{1}{2}$. Most recently, Roy & Pal (2014) measured a HI absorption distance using known anomalous velocity features near the Galactic Centre (GC) and found a lower limit on G1.9+0.3 distance from Sun as 10 kpc, some 2 kpc further away from the GC. Therefore, multiple radio observations have confirmed that G1.9+0.3 has the smallest angular diameter for a known Galactic SNR, indicative of its young age.

Green et al. (2008) re-observed G1.9+0.3 at 4.86 GHz using the VLA after Reynolds et al. (2008) used 2007 *Chandra* images to show G1.9+0.3 had expanded significantly since 1985 and its X-ray emission appeared to be predominantly synchrotron in nature. By comparing these new VLA observations with the 1985 VLA observations made at 1.49 GHz, Green et al. (2008) determined that G1.9+0.3 had expanded by $15\% \pm 2\%$ over 23 years ($\sim 0.65\%$ per year). Using the same VLA observations from 1985 and 1989, Gómez & Rodríguez (2009) derived an expansion rate of $0.46\% \pm 0.11\%$ and an age of 220^{+70}_{-45} years. By comparing 2007 and 2009 *Chandra* X-ray images and utilising a simple uniform-expansion model, Carlton et al. (2011a,b), find an expansion rate of $0.642\% \pm 0.049\% \text{ yr}^{-1}$ and a flux increase of $1.7\% \pm 1.0\% \text{ yr}^{-1}$, ageing the remnant at 156 ± 11 yr assuming no deceleration. Murphy, Gaensler & Chatterjee (2008) found that G1.9+0.3's flux density at 843 MHz increased by $1.22^{+0.24}_{-0.16}\%$ per year over

the last two decades.

Borkowski et al. (2013) suggest that G1.9+0.3 was likely a Type Ia SNe with the shell of its remnant in free expansion with a velocity $\sim 18000 \text{ km s}^{-1}$. The ejecta shows spatial asymmetry with prominent Fe-group elements in the northern rim. Also, we point out that Abramowski et al. (2014) report no γ -ray signal from G1.9+0.3 using observations from the H.E.S.S. (High Energy Stereoscopic System) Cherenkov telescope array.

The presence of polarised emission and spatial spectral variations are identified by Farnes (2012), with flatter spectra identified in the NW and SE of the remnant.

In this paper, we present the results of our Australia Telescope Compact Array (ATCA) radio-continuum observations of G1.9+0.3 made at 20, 13 & 6 cm in 2009. A comprehensive expansion study is conducted by comparing the new 6-cm observations with a previously unpublished 6-cm ATCA radio-continuum observation, made in 1993, and three 6-cm VLA observations made in 2008, 1989 and 1984 respectively. Here, we also report, on the radio-continuum spectral energy distribution and polarisation properties of this young SNR.

2. OBSERVATIONAL DATA

G1.9+0.3 was observed at 20, 13 & 6 cm wavelengths on four days in 2009 (Project C1952). Two of those days being in January 2009 with the remainder in February 2009. The 20-cm and 13-cm observations taken on the 2nd and 3rd day, were carried out simultaneously as they make use of a common feed-horn. The 6-cm observations taken on the 1st and 4th day, used four different frequencies (two per day) to improve multi-frequency synthesis (MFS). For this purpose, the MIRIAD (Sault & Killeen 2008) task MFPLAN was used to select the most appropriate frequencies. Over the four days G1.9+0.3 was observed with two separate antenna configurations for a total of 29 independent baselines covering a range of spacings from 31 to 6000 m. See Table 1 for complete observational details.

Table 1. 2009 ATCA observations of G1.9+0.3.

	Day 1	Day 2	Day 3	Day 4
Date	03 Jan	04 Jan	06 Feb	07 Feb
ATCA Array	6C	6C	EW352	EW352
Frequency 1	4.672 GHz	1.384 GHz	1.384 GHz	4.544 GHz
Frequency 2	5.440 GHz	2.368 GHz	2.368 GHz	5.184 GHz
Bandwidth	128 MHz	128 MHz	128 MHz	128 MHz
Time on source	332 min	458 min	509 min	1033 min
Primary Calibrator	J1934-638	J1934-638	J1934-638	J1934-638
Secondary Calibrator	J1741-312	J1751-253	J1751-253	J1741-312

¹Spectral index defined as $S \propto \nu^\alpha$

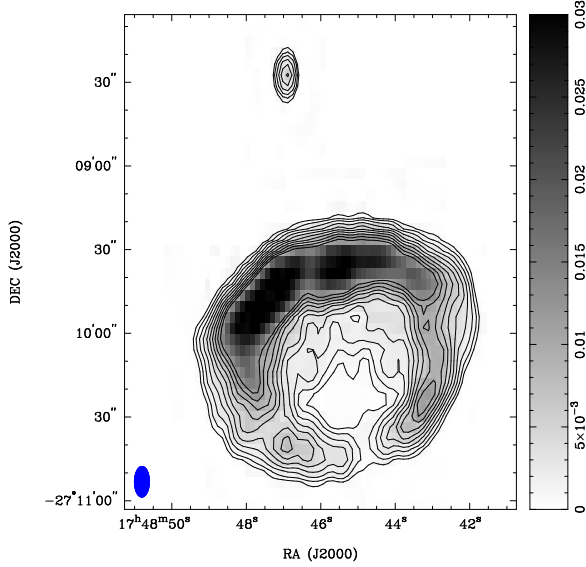


Fig. 1. ATCA 20-cm image of Galactic SNR G1.9+0.3. The blue ellipse in the lower left corner represents the synthesised beam of $10''.9 \times 5''.4$ at $PA = -0^\circ.5$. Contours are drawn at 3σ , 5σ , 8σ , 12σ , 17σ , 23σ , 30σ , 38σ , 47σ & 57σ ($\sigma = 0.22$ mJy/beam)

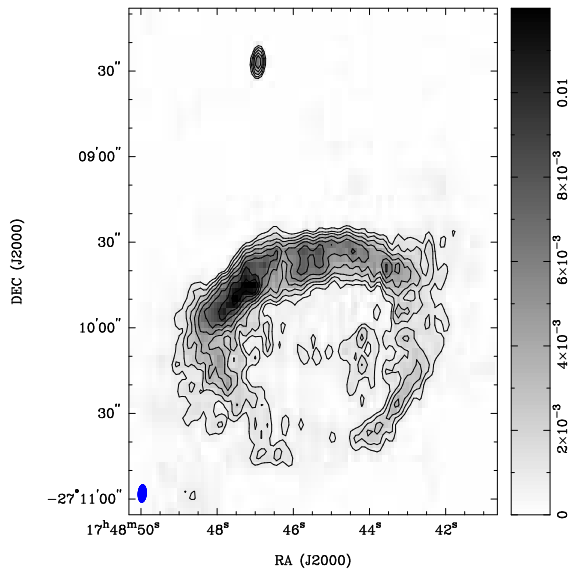


Fig. 2. ATCA 13-cm image of Galactic SNR G1.9+0.3. The blue ellipse in the lower left corner represents the synthesised beam of $6''.1 \times 2''.9$ at $PA = -0^\circ.5$. Contours are drawn at 3σ , 5σ , 8σ , 12σ , 17σ , 23σ , 30σ , 38σ , 47σ & 57σ ($\sigma = 0.32$ mJy/beam)

In Figs. 1 through 3 we show our new ATCA 2009 images of G1.9+0.3 at 20-cm, 13-cm and 6-cm respectively. All these images were formed using MFS with uniform weighting and were deconvolved using the MIRIAD (Sault & Killeen 2008) CLEAN and RESTOR tasks, with self calibration being applied to

the 6-cm image only. We note that our corresponding ATCA flux density measurements are significantly smaller ($\sim 50\%$) than the VLA estimates of Green et al. (2008). We can attribute this large difference to missing short spacings and poorer uv coverage of the ATCA images.

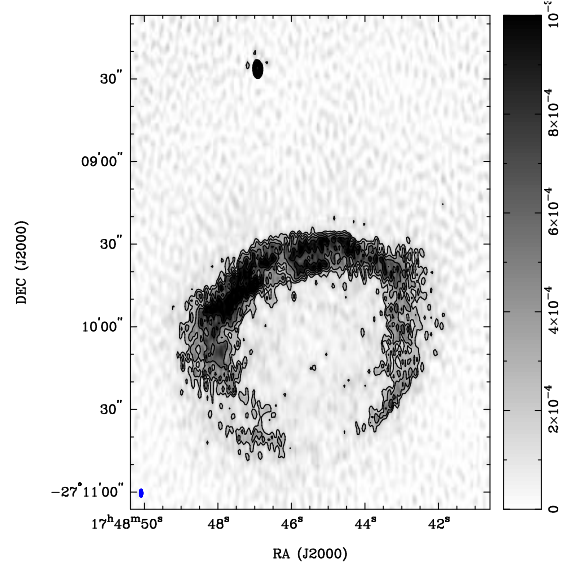


Fig. 3. ATCA 6-cm image of Galactic SNR G1.9+0.3. The blue ellipse in the lower left corner represents the synthesised beam of $2''.8 \times 1''.2$ at $PA = -0^\circ.5$. Contours are drawn at 3σ , 5σ , 8σ , 12σ , 17σ , 23σ , 30σ , 38σ , 47σ & 57σ ($\sigma = 0.07$ mJy/beam)

3. RESULTS

3.1 G1.9+0.3 Expansion and Age

A simple way to determine the age (in years) of a young SNR is to compare two images of the SNR taken at different epochs and to measure the percentage expansion the SNR has undergone over the time between the observations. Since we know that the SNR will have expanded by 100% in the intervening period between the SN explosion and the later observation, we can apply the simple formula, $Age = 100\%/ER$, where ER is the percentage expansion the SNR has undergone over the time between the observations (in years).

Ideally, to most accurately determine the expansion rate of an SNR, one should compare images from similar observations i.e., at the same wavelength and having similar, if not identical uv -coverage, resolution and rms noise.

In the case of G1.9+0.3 the first observations were made in 1984 using the VLA, with the best image produced from the 6 cm data (Fig. 4, bottom left). With this in mind, ATCA and VLA archives

Table 2. VLA observations of G1.9+0.3.

	1984 obs.	1989 obs.	2008 obs.
Date	26 May 1984	23 June 1989	12 March 2008
VLA Array	C	BC	C
Frequency	4.89 GHz	4.89 GHz	4.89 GHz
Bandwidth	50 MHz	50 MHz	50 MHz
Time on source	~10 min	~10 min	~30 min
Primary Calibrator	3C286	3C286	3C286
Secondary Calibrator	J1832-105	J1751-253	J1751-253

were searched for all available radio-continuum data of G1.9+0.3 made at this same wavelength — 6-cm.

For the expansion study carried out in this paper, one ATCA and three VLA observations made at 6-cm were found at different epochs from the original 1984 to 2008.

The archival ATCA observation were taken on the 10th June 1993 (Project C034; P.I.: A. Gray). This observation was made in the 6-cm band centred at 4672 and 5440 MHz with a bandwidth (BW) of 128 MHz and the telescope in 6A configuration². Source 1934-638 was used for primary calibration and source 1748-253 was used for secondary calibration. The observations were done in so-called “snap-shot” mode, totalling ~1 hour of integration spread equally over a 12 hour period. With very few short baselines and poor *uv*-coverage, resulting *rms* of 0.2 mJy beam⁻¹ is the highest amongst all the analysed observations. Consequently, the data for this observation are of very poor quality and while the results are presented here, we exclude measurements from this image in our determination of expansion rates and age.

The archival VLA observations were from the 1984 (Project AG0146), 1989 (Project AB0544) and 2008 (project AG0793), see Table 2 for details.

All these observations of G1.9+0.3 were reduced and analysed with the MIRIAD (Sault, Teuben & Wright 1995) and KARMA (Gooch 1995) software packages.

As the resolutions of the produced images varied (due to the various array configuration, observational periods and therefore resultant *uv*-coverage) the resolutions of all the images were smoothed/convolved to match the image with the

lowest resolution ($9'' \times 4''$ at a PA of 0°), see Fig. 4.

Since the *rms* noise of the resultant images also varied (see Table 3), it was decided not to try and determine the expansion by looking at how the shock front moved between epochs, but by looking at how the radially averaged shell profile peak moved from epoch to epoch.

Using RA=17^h48^m45.4^s, Dec=-27°10'06'' as the centre of G1.9+0.3 we produced normalised shell profiles (Fig. 5), averaged over all angles, for each of the images shown in Fig. 4.

Table 3. G1.9+0.3 *rms* noise (1σ) of 6 cm images shown in Fig. 4. All five images shown in Fig. 4 have matched resolution of $9'' \times 4''$ at a PA of 0° .

Telescope	Date	Image <i>rms</i> (mJy/beam)
VLA	1984	0.09
VLA	1989	0.09
ATCA	1993	0.20
VLA	2008	0.06
ATCA	2009	0.06

From the shell profiles in Fig. 5 we have determined the expansion rate in arc-seconds per year, percentage expansion per year, the averaged expansion velocity in km s⁻¹ (assuming a distance of 8.5 kpc³), and age in years. These results are summarised in Tables 4 through 7 respectively.

²We combined these two frequencies into a single 1 GHz band, see image shown in Fig. 4 (middle left).

³Distance estimates to G1.9+0.3 vary between ~7.8 kpc (Nord et al. 2004) and 10 kpc (Roy & Pal 2014). We use 8.5 kpc as the most likely distance – suggested by Reynolds et al. (2008).

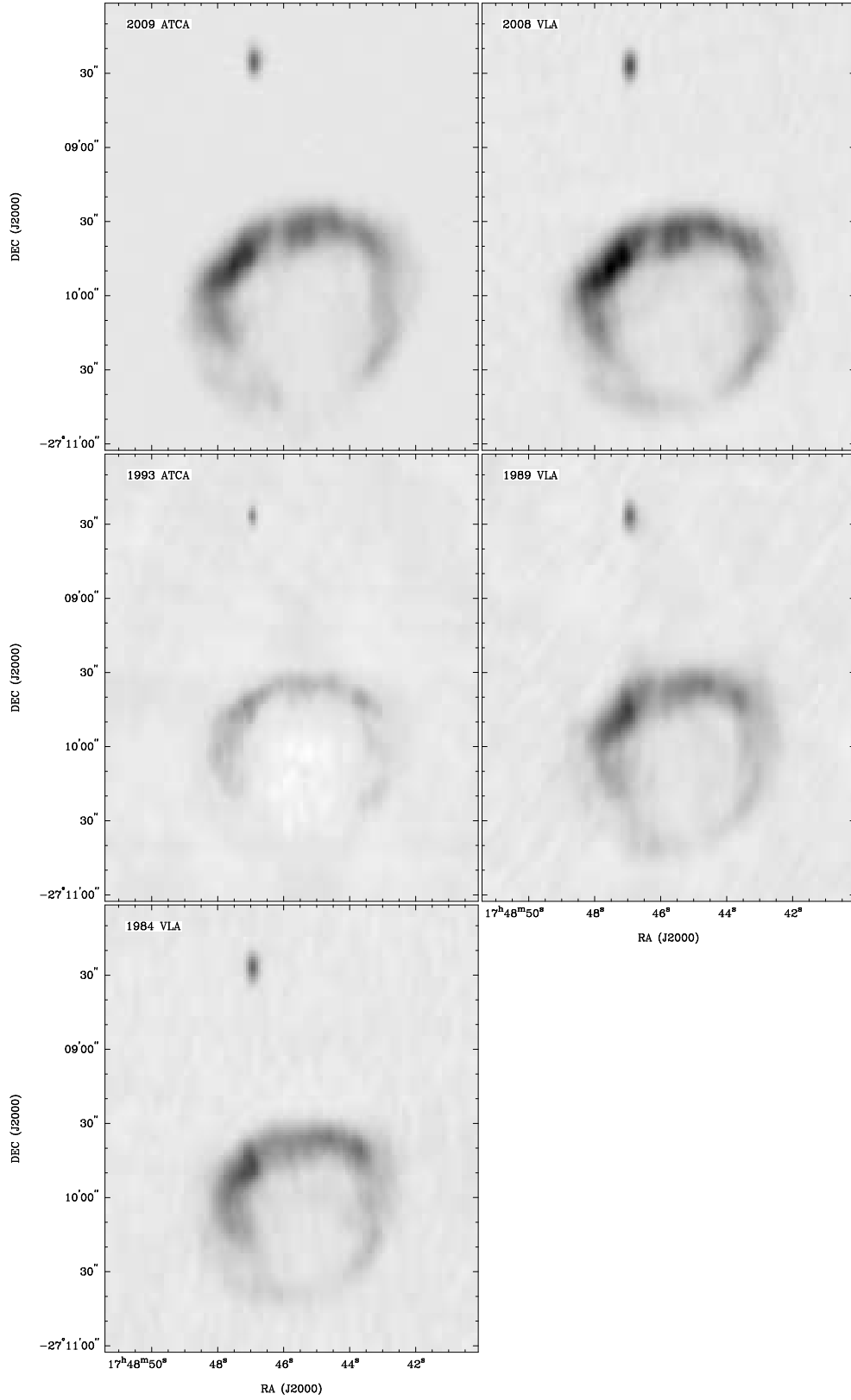


Fig. 4. Matched resolution ($9'' \times 4''$ at a PA of 0°) 6-cm images of Galactic SNR G1.9+0.3 (centred at $RA(J2000)=17^h 48^m 45.4^s$, $Dec(J2000)=-27^\circ 10' 06''$) at multiple epochs. Left to right, top to bottom, 2009 ATCA, 2008 VLA, 1993 ATCA, 1989 VLA & 1984 VLA.

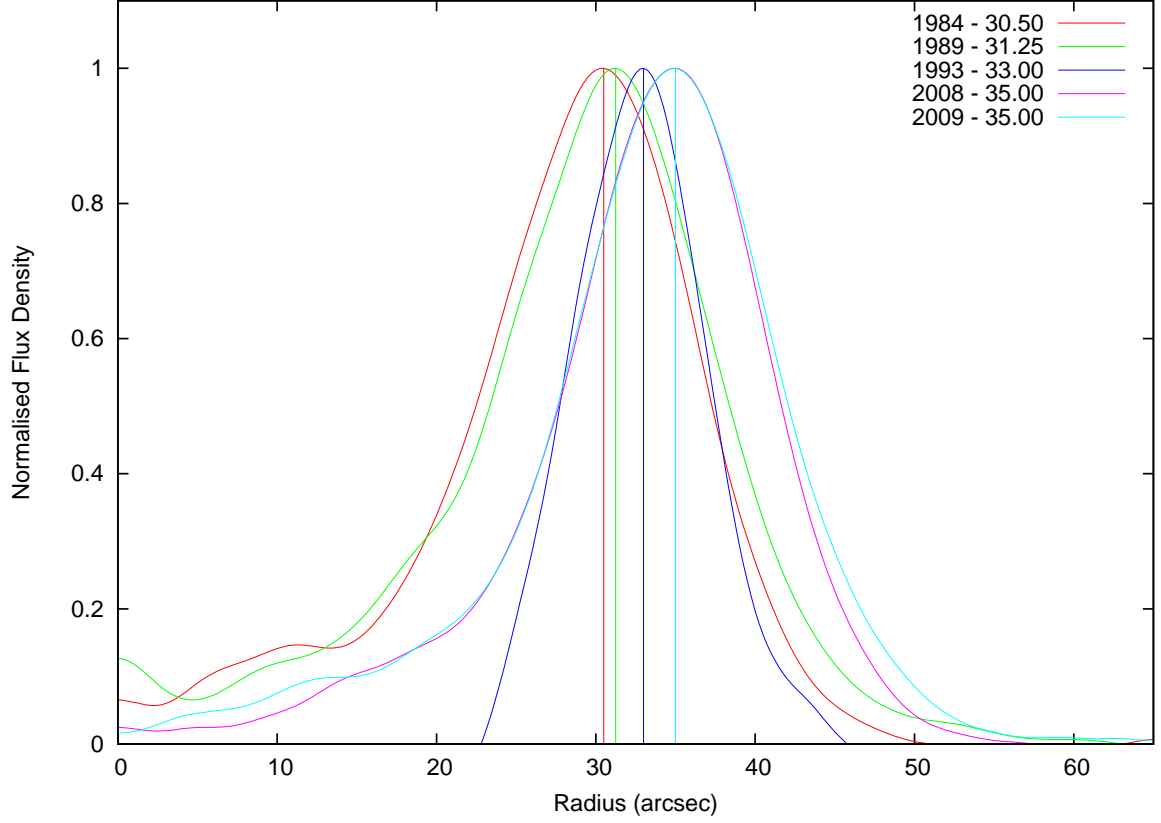


Fig. 5. Normalised shell profiles averaged over all angles for each image of G1.9+0.3 in Fig. 4.

Table 4. Expansion rate of G1.9+0.3 in arc-seconds per year of radially averaged radio-continuum emission peak.

	1984	1989	2008	2009
1984	0			
1989	0.148	0		
2008	0.189	0.200	0	
2009	0.182	0.191	0	0

Table 5. % Expansion of G1.9+0.3 per year of radially averaged radio-continuum emission peak.

	1984	1989	2008	2009
1984	0			
1989	0.484	0		
2008	0.620	0.641	0	
2009	0.598	0.612	0	0

Table 6. Estimated age of G1.9+0.3 in years.

	1984	1989	2008	2009
1984	0			
1989	206	0		
2008	161	156	0	
2009	167	163	0	0

Table 7. Speed of radially averaged radio-continuum emission peak in km s^{-1} of G1.9+0.3.

	1984	1989	2008	2009
1984	0			
1989	5 950	0		
2008	7 620	8 070	0	
2009	7 350	7 710	0	0

In Tables 4 and 5 we show the expansion of G1.9+0.3 over the period between 1984 and 2009. The median expansion over this period (excluding the 1993 observations) is $0.563\% \pm 0.078\% \text{ yr}^{-1}$ or $0.174 \pm 0.026 \text{ arcsec yr}^{-1}$. However, we note that between 1984 and 1989, G1.9+0.3 expanded at a somewhat slower rate ($0.484\% \text{ yr}^{-1}$) which was also esti-

mated by Gómez & Rodríguez (2009) at $0.46\% \pm 0.11\%$ based on 20-cm VLA data from the same period. Since 1989, G1.9+0.3 appears to expand at a faster rate of up to 0.641% per year which is in excellent agreement with the X-ray estimates of Carlton et al. (2011a,b) of $0.642\% \pm 0.049\%$ and Green et al. (2008) using VLA observations. This may be an indication that perhaps the shock has “broken through” to a region of lower density and thus accelerated. The median expansion rate derived here, yields an upper age limit of 181 ± 25 years (Table 6) assuming a constant expansion rate since the SN event. This dates the SN event back to the year 1828 (± 25).

Similarly, the speed at which the radially averaged radio-continuum emission peak is moving (assuming a distance to G1.9+0.3 of 8.5 kpc) is

somewhat slower in the 1980’s ($\sim 6000 \text{ km sec}^{-1}$) than later when it speeds up to $\sim 8000 \text{ km sec}^{-1}$ (Table 7). The speed of radially averaged radio-continuum emission peak should not be confused with the expansion velocity of the SNR shock front, which has been estimated at $\sim 18000 \text{ km sec}^{-1}$ by Borkowski et al. (2013).

As our determination of the radially averaged radio-continuum emission peak speed is dependent on the distance to the SNR we estimate that at the lower end (between 1984 and 1989) the speed varies between 5500 km sec^{-1} (at a distance of 7.8 kpc) and 7000 km sec^{-1} (at a distance of 10 kpc). More recently (between 1989 and 2009), the speed varies between 7400 km sec^{-1} (at a distance of 7.8 kpc) and 9500 km sec^{-1} .

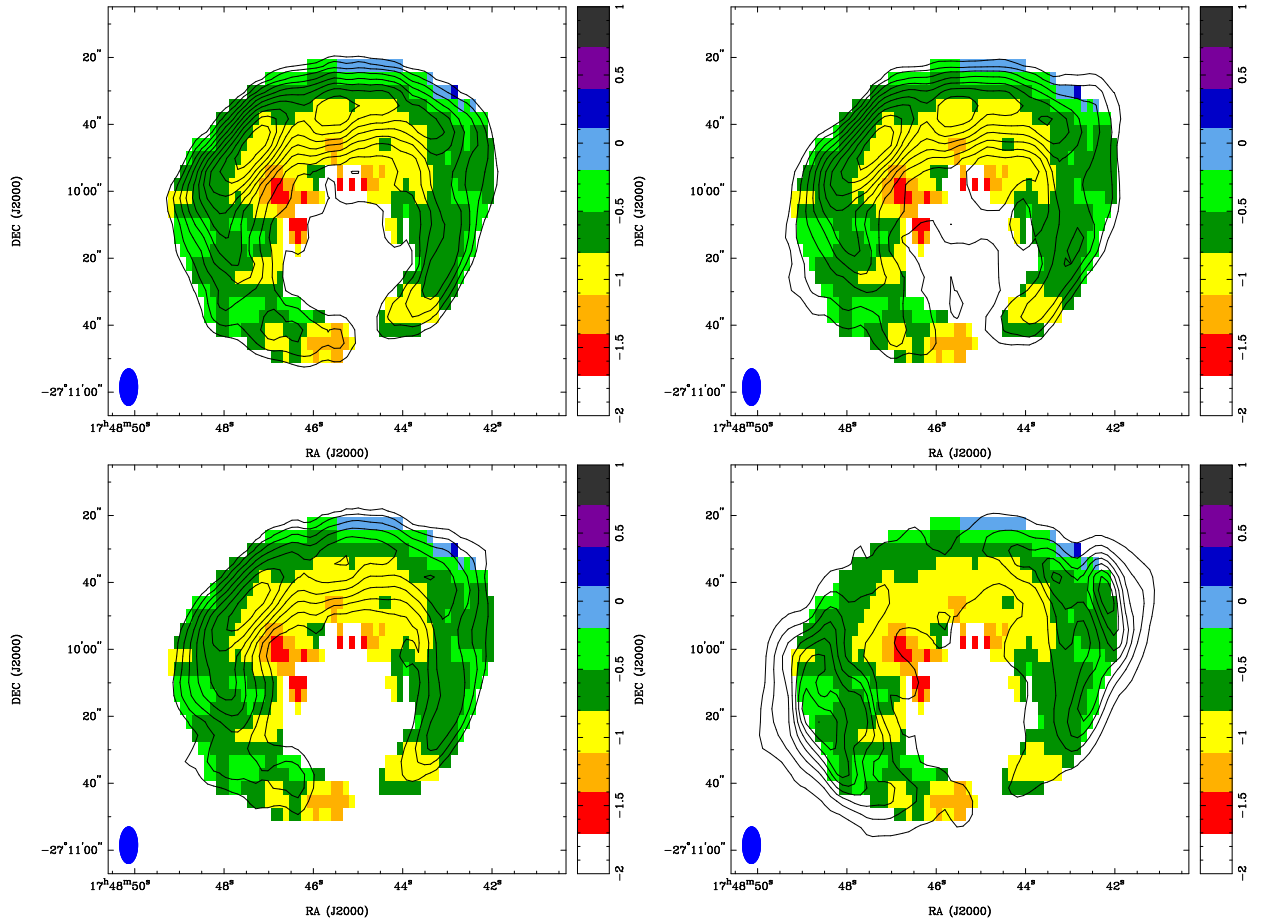


Fig. 6. The Spectral Index map of G1.9+0.3 overlaid with 20-cm contours (top left; contours are: 3, 5, 8, 12, 12, 17, 23, 30, 38, 47, $57 \times 7.5 \times 10^{-4} \text{ Jy/beam}$), 13-cm contours (top right; contours are: 3, 5, 8, 12, 17, 23, 30, 38, 47, $57 \times 6.0 \times 10^{-4} \text{ Jy/beam}$), 6-cm contours (bottom left; contours are: 3, 5, 8, 12, 17, 23, 30, $5.0 \times 10^{-4} \text{ Jy/beam}$) and 2007 Chandra X-ray contours (bottom right; contours are: 33.57, 67.14, 100.7, 134.3, 167.9, 201.4, 235, 268.6 cts/s).

3.2 G1.9+0.3 Spectral Energy Distribution

By matching the resolutions of our 2009 ATCA images at 6-cm and 13-cm to that of the 20-cm image ($10''.9 \times 5''.4$ at $PA = -0^\circ.5$), a three point spectral index map was created, allowing for the examination of the spatial spectral variations in the remnant (see Fig. 6). In this map, the colour of each pixel represents the spectral index α across the three observational frequencies.

From this map we can see that the radio-continuum spectral energy distribution across the NW and SE regions is flatter ($\alpha \sim -0.5$) which is also following the contours of the strongest of X-ray emission (so called “X-ray ears” of G1.9+0.3; see Fig. 6 – bottom right). This SED flattening in the NW and SE is also confirmed by Farnes (2012) in his VLA observations. The steeper ($\alpha \sim -1$) radio spectra is dominant in the Northern region of G1.9+0.3 corresponding to where the radio emission is the strongest images and therefore indicating synchrotron radio-continuum emission. We also note that somewhat steeper spectral index ($\alpha < -1.0$) is dominating inside part of the SNR while flatter spectra is at the edges.

We estimate that the average spectral index across the entire SNR is $\alpha = -0.72 \pm 0.26$ which is flatter than LaRosa et al. (2000) ($\alpha = -0.93 \pm 0.25$), however, their estimates are based on 20/90 cm flux density measurements. This may indicate that the synchrotron emission may even more dominant at higher wavelengths (92 cm). Using Green et al. (2008) flux density estimates at 20 and 6 cm from their 2008 VLA observations we estimate spectral index of $\alpha = -0.62 \pm 0.08$ which is in good agreement with our ATCA estimates from approximately one year later. This steeper spectral index is expected for younger SNRs (Bell et al. 2011) and further confirms its young age.

3.3 Polarisation of G1.9+0.3

Since the ATCA observations recorded Stokes parameters Q , U and V , in addition to total intensity I , we were able to determine the polarisation of G1.9+0.3. In our 6 cm image (Fig. 7) we show the regions of polarised emission for G1.9+0.3. The electric field vectors follow the shell of the SNR around most of the circumference of the SNR, particularly along its eastern side.

The maximum fractional polarisation is estimated to be $P = 17 \pm 3\%$ with a mean of 6%. No reliable polarisation was detected at 20 or 13 cm. This might indicate significant depolarisation in the remnant, however the polarimetric response of the ATCA is known to be poor at 13-cm.

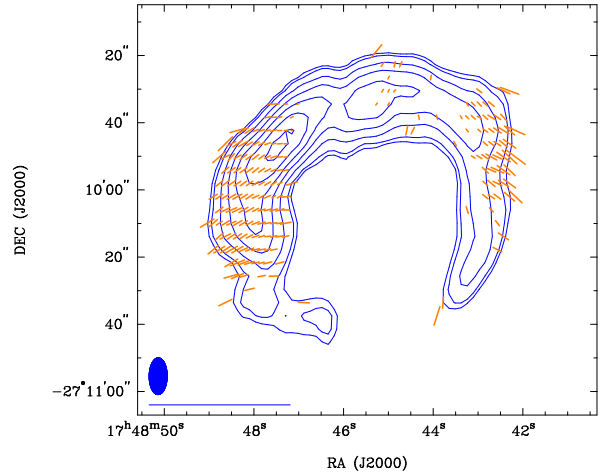


Fig. 7. 6-cm ATCA observations of G1.9+0.3. The blue ellipse in the lower-left corner represents the synthesised beam width of $10''.940 \times 5''.384$ at $PA = -0^\circ.5$. The length of the vectors represents the fractional polarised intensity at each pixel position, and their orientations indicate the mean PA of the electric field (averaged over the observing bandwidth, not corrected for any Faraday rotation). The blue line below the beam ellipse represents the length of a polarisation vector of 100%. The maximum fractional polarisation is $17\% \pm 3\%$ with a mean of 6%. Contours at 2.2, 2.8, 4.4, 6.6, 9.4, 13, 17, 21, 26 and 32 mJy beam $^{-1}$.

Typically, young type Ia SNRs exhibit a radially oriented magnetic field (tangentially oriented electric field), which is to be expected from Rayleigh-Taylor instabilities in a decelerating remnant (Gull 1975; Chevalier 1976). This is consistent with similarly young Galactic SNRs, as well as in the LMC (e.g. Table 3 in Bozzetto et al. (2014)). As we have plotted electric field vectors we would expect that they would be tangential to the circumference of the remnant. We can see in Fig. 7, the orientation of the electric field vectors roughly follow this arrangement, however it can be seen that this pattern is not strictly followed around the entire remnant. Given the location of G1.9+0.3, towards the Galactic centre, this is most likely due to Faraday depolarisation.

Farnes (2012) also detected the presence of polarised emission. Our ATCA polarimetric results also suggest that the above observed variation is most consistent with an ambient B field perpendicular to the axis of bilateral symmetry indicated by Farnes (2012). Moreover, Farnes (2012) argues that increased ordering of the B field in the NW as the strong Faraday depolarisation must also be present.

Farnes (2012), also argues that an intrinsically radially-oriented field could be provided by a systematic gradient in Rotation Measure (RM) of 140 rad m^{-2} from N to S and can also explain the depolarisation that we observe in our ATCA images (see Sect. 3.3).

3.4 Magnetic Field of G1.9+0.3

We used the new equipartition formulae derived by Arbutina et al. (2012, 2013) based on the diffusive shock acceleration (DSA) theory of Bell (1978) to estimate a magnetic field strength. These formulae are particularly relevant to magnetic field estimation in SNRs, and yields magnetic field strengths between those given by the classical equipartition (Pacholczyk 1970) and revised equipartition (Beck and Krause, 2005) methods. We estimate the magnetic field strength of G1.9+0.3 to be $B \approx 273 \mu\text{G}$ and the minimum total energy of the synchrotron radiation to be $E_{\min} \approx 1.8 \times 10^{48}$ ergs (see Arbutina et al. (2012, 2013)); and corresponding online calculator⁴). For this estimate, we used a spectral index value of $\alpha = -0.72$, integrated flux density $S_{1.425} = 0.935$ Jy at $\nu = 1.425$ GHz (Green et al. 2008), distance $D = 8.5$ kpc, SNR radius of $r = 46''$ and filling factor of 0.33. However, if we additionally assume shock velocity of 18000 km s^{-1} (as suggested by Borkowski et al. (2013)) than the magnetic field strength of G1.9+0.3 becomes somewhat lower ($B \approx 180 \mu\text{G}$ and the minimum total energy of the synchrotron radiation is $E_{\min} \approx 7.6 \times 10^{47}$ ergs. These estimates are very similar to Arbutina et al. (2012) estimates of $B \approx 228 \mu\text{G}$ and $E_{\min} \approx 9.3 \times 10^{47}$ ergs.

A large magnetic field strength such as this ($273 \mu\text{G}$), is expected for a young SNR (Bell 2004). Indeed, this makes G1.9+0.3, a remnant with one of the the strongest estimated magnetic field strengths known to date. For example, other young Galactic SNRs (Beck & Krause 2005; Arbutina et al. 2012 (see their Table 1)) such as Cas A ($B \approx 1250 \mu\text{G}$), Kepler ($B \approx 414 \mu\text{G}$), G349.7+0.2 ($B \approx 523 \mu\text{G}$) and Tycho ($B \approx 285 \mu\text{G}$) are known remnants with the strongest magnetic fields. Also, in a Large Magellanic Cloud (LMC) SNR, J0509-6731 (also remnant from a Type Ia SN explosion) at about 400 yrs age has magnetic field strength of $168 \mu\text{G}$ (Bozzetto et al. 2014) while the magnetic field of LMC SNR J0519-6902 is $171 \mu\text{G}$ (Bozzetto et al. 2012). The Small Magellanic Cloud SNR HFKP 443 (Crawford et al. 2014, in press) has a field strength of $90 \mu\text{G}$ with numerous other older remnants falling below these values. It is most likely that G1.9+0.3 is going through an evolutionary stage where the magnetic field has been amplified (added to simple compression by the shocks), which may explain such a high magnetic field value (Telezhinsky et al. 2012). The amplification of magnetic field is a process driven by the very fast shocks of young SNRs. Because of strong amplification of magnetic field, a spectral index of $\alpha = -0.72$ and the location in the surface brightness-diameter diagram this SNR is of younger age, in free expansion stage and expanding in somewhat denser environment ($\sim 3 \text{ cm}^{-3}$).

In Fig. 8 we show a surface brightness–

diameter ($\Sigma - D$) diagram at 1 GHz with theoretically-derived evolutionary tracks (Berezhko & Völk 2004) superposed. G1.9+0.3 lies at $(D, \Sigma) = (3.8 \text{ pc}, 1.3 \times 10^{-17} \text{ W m}^{-2} \text{ Hz}^{-1} \text{ Sr}^{-1})$ on the diagram. Its position tentatively suggests that it is in the mid-to-late free expansion phase of evolution — expanding into a somewhat denser environment with the canonical initial energy of a supernova explosion (10^{51} ergs).

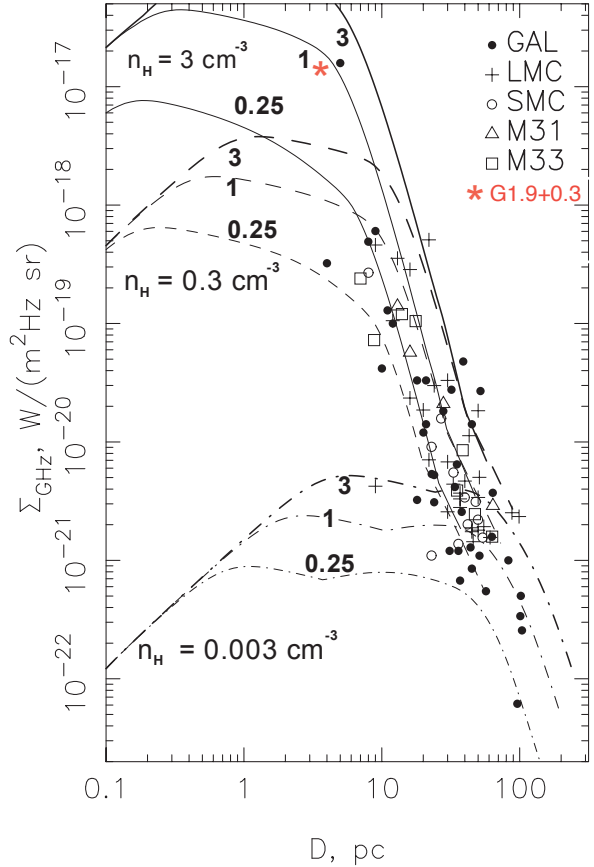


Fig. 8. 1 GHz Surface brightness-to-diameter diagram from Berezhko & Völk (2004), with G1.9+0.3 added. The evolutionary tracks are for ISM densities of $N_H = 3, 0.3$ and 0.003 cm^{-3} and explosion energies of $E_{\text{SN}} = 0.25, 1$ and $3 \times 10^{51} \text{ erg}$.

⁴<http://poincare.matf.bg.ac.rs/~arbo/eqp/>

4. CONCLUSIONS

Here, we have presented new 6-cm, 13-cm and 20-cm ATCA observation of Galactic SNR G1.9+0.3 made in 2009. Using the new 6-cm data and archival 6-cm data, we observe that there are indications that the expansion of G1.9+0.3 accelerated after 1989. Our results are in broad agreement with the estimates of expansion made by Reynolds et al. (2008), Green et al. (2008), Gómez & Rodríguez (2009) and Carlton et al. (2011a,b). We find that at ~ 181 yrs, G1.9+0.3 is indeed very young and most likely the youngest SNR in the Milky Way. This very young age is also reinforced by magnetic field arrangement and strength we estimate.

We make the following findings:

- Expansion rate of 0.484% per year between 1984 and 1989;
- Expansion rate of 0.641% per year between 1989 and 2009;
- Median expansion rate of $0.563\% \pm 0.078\%$ per year between 1984 and 2009;
- Age of $181 \text{ yrs} \pm 25 \text{ yrs}$;
- Average spectral index between 20-cm and 6-cm, across the entire SNR is $\alpha = -0.72 \pm 0.26$;
- 6% fractionally polarised radio emission with a peak of $17\% \pm 3\%$;
- Magnetic field strength $B \approx 273 \mu\text{G}$;

Acknowledgements – We used the KARMA and MIRIAD software package developed by the ATNF. The Australia Telescope Compact Array is part of the Australia Telescope which is funded by the Commonwealth of Australia for operation as a National Facility managed by CSIRO. The Karl G. Jansky Very Large Array (VLA). The National Radio Astronomy Observatory is a facility of the National Science Foundation operated under cooperative agreement by Associated Universities, Inc.

REFERENCES

- Abramowski, A. and H. E. S. S. Collaboration et al.: 2014, *Mon. Not. R. Astron. Soc.*, **441**, 790.
- Arbutina B., Urošević D., Andjelić M. M., Pavlović, M. Z., Vukotić B.: 2012, *Astrophys. J.*, **746**, 79.
- Arbutina B., Urošević D., Vučetić M. M., Pavlović, M. Z., Vukotić B.: 2013, *Astrophys. J.*, **777**, 31.
- Beck, R., and Krause, M.: 2005, *Astron. Nachr.*, **326**, 414.
- Bell, A. R.: 1978, *Mon. Not. R. Astron. Soc.*, **182**, 443.
- Bell, A. R.: 2004, *Mon. Not. R. Astron. Soc.*, **353**, 550.
- Bell, A. R., Schure K. M., Reville B.: 2011, *Mon. Not. R. Astron. Soc.*, **418**, 1208.
- Berezhko, E. G. and Völk, H. J.: 2004, *Astron. Astrophys.*, **427**, 525.
- Borkowski, K. J., Reynolds, S. P., Hwang, U., Green, D. A., Petre, R., Krishnamurthy, K. and Willett, R.: 2013, *Astrophys. J.*, **771**, L9.
- Bozzetto, L. M., Filipović, M. D., Urošević, D. and Crawford, E. J.: 2012, *Serb. Astron. J.*, **185**, 25.
- Bozzetto, L. M., Filipović, M. D., Urošević, D., Kothes, R. and Crawford, E. J.: 2014, *Mon. Not. R. Astron. Soc.*, **440**, 3220.
- Cappellaro, E.: 2003, in "Supernovae and Gamma-Ray Bursters", ed. Weiler K., Lecture Notes in Physics, Berlin Springer Verlag, Vol. **598**, 37.
- Carlton, A. K., Borkowski, K. J., Reynolds, S. P., Willett, R., Krishnamurthy, K., Green, D. A. and Petre, R.: 2011a, in American Astronomical Society Meeting Abstracts 217. p. 256.12.
- Carlton, A. K., Borkowski, K. J., Reynolds, S. P., Hwang, U., Petre, R., Green, D. A., Krishnamurthy, K. and Willett, R.: 2011b, *Astrophys. J.*, **737**, L22.
- Chevalier, R. A.: 1976, *Astrophys. J.*, **207**, 872.
- Farnes, J.: 2012, PhD thesis, University of Cambridge.
- Gooch, R. E.: 1995, in Astronomical Data Analysis Software and Systems IV, ASP Conf. Series ed. Shaw, R. A., Payne, H. E. and Hayes, J. J. E., **77**, 144.
- Gray, A. D.: 1994, *Mon. Not. R. Astron. Soc.*, **270**, 835.
- Green, D. A. and Gull, S. F.: 1984, *Nature*, **312**, 527.
- Green, D. A.: 2004, *Bull. Astr. Soc. India*, **32**, 335.
- Green, D. A., Reynolds, S. P., Borkowski, K. J., Hwang, U., Harrus, I. and Petre, R.: 2008, *Mon. Not. R. Astron. Soc.*, **387**, L54.
- Gómez, Y. and Rodríguez, L. F.: 2009, *Rev. Mex. Astron. Astrofis.*, **45**, 91.
- Gull, S. F.: 1975, *Mon. Not. R. Astron. Soc.*, **171**, 263.
- LaRosa, T. N., Kassim, N. E., Lazio, T. J. W. and Hyman, S. D.: 2000, *Astron. J.*, **119**, 207.
- Murphy, T., Gaensler, B. M., Chatterjee, S.: 2008, *Mon. Not. R. Astron. Soc.*, **389**, L23.
- Nord, M. E., Lazio, T. J. W., Kassim, N. E., Hyman, S. D., LaRosa, T. N., Brogan, C. L. and Duric, N.: 2004, *Astron. J.*, **128**, 1646.
- Pacholczyk, A. G.: 1970, in "Radio astrophysics.

- Nonthermal processes in galactic and extragalactic sources", ed. A. G. Pacholczyk (San Francisco: Freeman).
- Reynolds, S. P., Borkowski, K. J., Green, D. A., Hwang, U., Harrus, I. and Petre, R.: 2008, *Astrophys. J.*, **680**, L41.
- Reynolds, S. P., Borkowski, K. J., Green, D. A., Hwang, U., Harrus, I. and Petre, R.: 2009, *Astrophys. J.*, **695**, L149.
- Roy, S. and Pal, S.: 2014, in "Supernova environmental impacts", eds. Ray A. and McCray R. A., IAU Symposium Vol. **296**, 197.
- Sault, B. and Killeen, N.: 2008, Miriad Users Guide. Australia Telescope National Facility.
- Sault, R. J., Teuben, P. J. and Wright, M. C. H.: 1995, in "Astronomical Data Analysis Software and Systems IV ASP Conference Series", eds. Shaw, R. A., Payne, H. E. and Hayes, J. J. E., **77**, 433.
- Telezhinsky, I., Dwarkadas, V. V., and Pohl, M.: 2012, *Astropart. Phys.*, **35**, 300.
- van den Bergh, S. and Tammann, G. A.: 1991, *Annu. Rev. Astron. Astrophys.*, **29**, 363.

РАДИО КОНТИНУУМ ЕМИСИЈА МЛАДОГ
ГАЛАКТИЧКОГ ОСТАТКА СУПЕРНОВЕ G1.9+0.3

A. Y. De Horta¹, M. D. Filipović¹, E. J. Crawford¹, F. H. Stootman¹, T. G. Pannuti²,
L. M. Bozzetto¹, J. D. Collier¹, E. R. Sommer¹ and A. R. Kosakowski²

¹*University of Western Sydney, Locked Bag 1797, Penrith South, DC, NSW 1797, Australia*
E-mail: a.dehorta@uws.edu.au, m.filipovic@uws.edu.au, e.crawford@uws.edu.au

²*Space Science Center, Department of Earth and Space Sciences,
Morehead State University, 235 Martindale Drive, Morehead, KY 40351 USA*
E-mail: t.pannuti@moreheadstate.edu

UDK ...
Уређивачки прилог

У овој студији представљамо нова радио-континуум посматрања на 6 цм најмлађег остатка супернових (ОС) у нашој Галаксији. Остатак G1.9+0.3 је $\sim 181 \pm 25$ година стар и годишња стопа раста му је $0.563\% \pm 0.078\%$ у периоду између 1984 и 1989. Приметили смо да се између 1984 и 1989, остатак ширио нешто спорије (0.484% годишње) него после 1989-те када је експанзија

достигла ниво од 0.641% годишње. G1.9+0.3 има типичан радио-спектар за младе остатке са $\alpha = -0.72 \pm 0.26$. G1.9+0.3 емитује просечно 6% поларизованог зрачења на талсној дужини од 6 цм, са максималним интензитетом $17\% \pm 3\%$. Ова поларизациона емисија такође тесно прати рентгенско зрачење. Процењено је прилично јако магнетно поље у вредности од $273 \mu\text{G}$ што представља једно од најснажнијих магнетних поља у до сада посматраним ОС.